Proceedings World Geothermal Congress 2020+1
Reykjavik, Iceland, April - October 2021

Feed Zones Characterization Based on the Intensity of Faults and Fractures to Reduce the Uncertainty of the Future Field Development in Ulubelu Geothermal Field, Lampung, Indonesia

Muhammad Tajul Arifin, Imam M. Prasetyo, Graniko R. Pratama, Mochamad Husni Thamrin, Hary Koestono

PT. Pertamina Geothermal Energy

Menara Cakrawala 19th floor, Jl. M. H. Thamrin No.9, DKI Jakarta, 10430

Muhammad.tajul@pertamina.com

Keywords: Ulubelu, Semangko Fault, Feed Zones, Faults, Fractures

ABSTRACT

Located at the southern tip of Sumatra, geological structures in Ulubelu Geothermal Field strongly depicts the consequence of dextral movement of the Great Sumatran Fault along with the volcanic activity related structures. It produces northwest – southeast (NW-SE) alignments that can be clearly observed on the morphology. Although the NW-SE structures is obvious on the surface, how much the influence of these structures such as faults and fractures to the permeability in Ulubelu Geothermal Field is still uncertain. The study is conducted by integrating borehole image logging data with Production Logging Tool (PLT) from eight wells to assess the impact of these structures to the permeability of each feed zones.

The study reveals permeability of the feed zones can be divided further into four ranks based on the intensity of the faults and fractures. The predominantly northwest – southeast (NW-SE) faults and conductive fractures intersected by the wells are the main factor to the fluid flow contribution from the feed zones. It is evidenced that fault zone gives the highest flow contribution. When the fault is absent the permeability deteriorates and leaving the intensity of conductive fractures contributes to some degree, mainly contributes between a half and a third compared to the fault contribution. By plotting the feed zones elevation with its rank, the feed zones are located differently on the western and the eastern part of the field due to fault control. The identification of these feed zones and its controlling factor will greatly reduce the uncertainty for future field development and plan the effective make-up wells.

1. INTRODUCTION

A geothermal system could be found in an area around the dextral strike-slip fault movement forming pull-apart basin and the volcanic cluster (Muraoka, et al., 2010). The condition found in Ulubelu geothermal field is one of its example. The field is located at the southern tip of Sumatra Island near the termination of Sumatra Fault Zone (Figure 1). Therefore, its geological structure is influenced by both tectonic and volcanic activities. There are numerous faults and circular features as the result of tectono-volcanic activity.

Figure 1: Tectonic map of Sumatra showing the relative location of Ulubelu Geothermal Field (UGF) at the southern tip of Sumatra Fault Zone (SFZ) (modified from Muraoka, et al., 2010, Barber, et al., 2005, Darman & Sidi, 2000, Sieh & Natawidjaja, 2000).

The Ulubelu Geothermal Field (UGF) occupies 2-3 km wide depression with dominant NW-SE structures (Figure 2). These structures are parallel – sub parallel with the greater Semangko Fault (southern segment of SFZ). The occurrence of manifestation around the field is mainly associated with these NW-SE structures that provide permeability for ascending hydrothermal fluid to the surface. Evidence from UBL-03 and UBL-26 in Trianggo, et al., 2015 shows that the NW-SE fault and their associated fractures are the productive structures in the subsurface of Ulubelu.

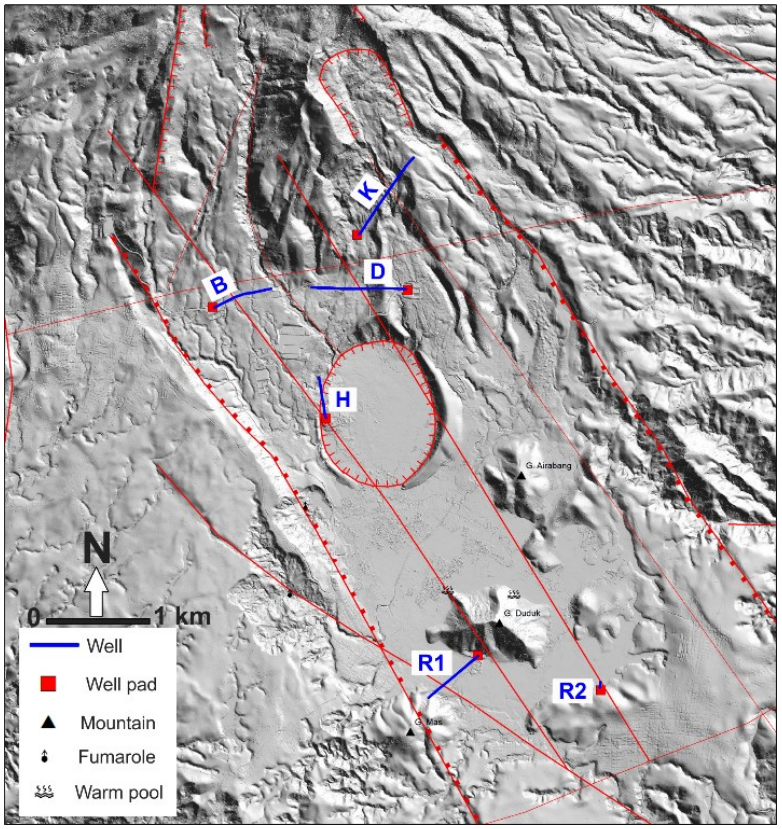

Figure 2: Geological structure of Ulubelu Geothermal Field dominated by NW-SE faults and some circular features. The trajectory of six wells that were used in this study.

Based on evidence from both surface and subsurface as explained above, we know faults and its associated fractures enhance the permeability of the existing rocks. Secondary permeability allows greater hydrothermal fluid to flow from subsurface to the surface. However, it is difficult to exactly quantify both structures contributing to the fluid flow in geothermal. The following chapters discuss the integration of borehole geology and reservoir data in UGF to reveal the effect of faults and fractures on permeability.

2. METHODOLOGY

Borehole image data and production logging tools (PLT) survey with heating up temperature profiles and drilling circulation from six wells were used for this study to assess the influence of faults and fractures to reservoir rocks permeability.

There are five types of sinusoidal feature that has been identified as fractures and fault on the borehole image data (Figure 3); (1) Continuous conductive fracture (CCF) is characterized by dark, brownish, blackish sinusoid that cuts across the borehole. (2) Discontinuous conductive fracture (DCF) is similar to CCF but it only partially cuts the borehole. (3) Low angle conductive fracture (LACF) is characterized by either continuous or discontinuous sinusoid with dark, brownish, blackish colour and has dip magnitude of $<30^{o}$. (4) Resistive fracture (RF) has bright or whitish sinusoid colour. (5) Fault (FA) is identified based on the washed out borehole due to intense fracturing that caused distorted image. Then the identified fractures were plotted based on depth and fracture strike to see the distribution on each well.

Conductive fracture exhibit darker colour on the image due to its low resistivity value. Several reasons could make that situation such as filled by conductive drilling mud if it is an open fracture, mineralized by pyrite or clay minerals. Meanwhile, the resistive fractures have brighter colour due to its higher resistivity value. Higher resistivity value occurs as the fracture filled by resistive minerals such as calcite, quartz or others.

Production logging tools (PLT) survey data is utilized to locate the depth of feedzones and flow contibutions from each entry. Minus percentage in the flow contribution reflects the flow from borehole into formation, while the positive percentage suggests that the flow runs from formation into the borehole. Fracture density (fracture/m) for four fractures type (CCF, DCF, LACF, RF) then were calculated by using the depth interval of each feed zone. Fault is excluded from the calculation of fracture density as it is rarely found and for practical reason in the plotting against contribution to separate fault with the other fractures. Feed zones with contribution <5% are also excluded from fracture density calculation. Moreover, fracture density and flow contribution were plotted to reveal the impact of fracture and fault to the permeability.

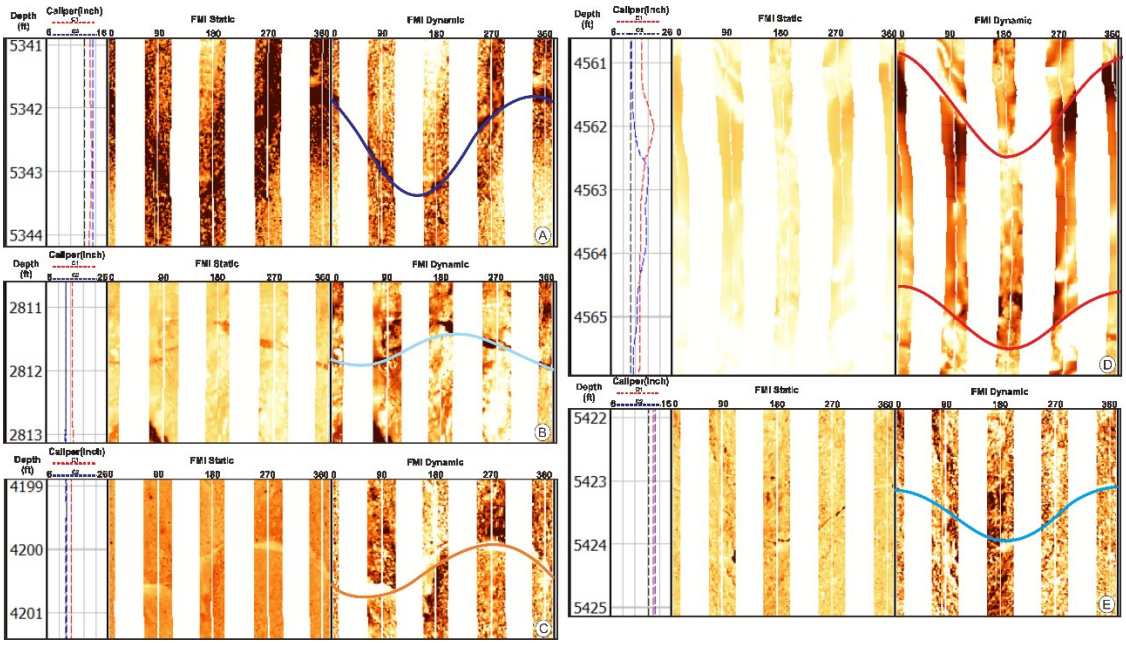

Figure 3: Five type of planar features on the borehole image data. (A) Continuous conductive fracture (CCF); (B) Low angle continuous conductive fracture (LACF); (C) Resistive fracture (RF); (D) Fault (FA); Discontinuous conductive fracture (DCF)

3. RESULTS & DISCUSSIONS

Thorough analysis has been made from the wells data. It shows the NW-SE fractures trend is predominating with dip direction either to the SW or SE. All the data is represented on elevation in meters above sea level (masl). Each well is reviewed below:

3.1 Well B

It could be seen on the chart below (Figure 4) this well is dominated by NW-SE fractures with SW dip azimuth. Feed zones with > 5% contribution were calculated its fracture density. The temperature profile does not give us insight about the location of feed zones as it was directly measured 128 days after the well completion.

From top to bottom borehole, resistive fractures took place from elevation 0 to -850 masl and covers two major feed zone. The occurrence of resistive fractures is often interpreted as sealed fractures due to deposition of resistive mineral (e.g. quartz, calcite). Although dominated by resistive fracture, on the interval of two major feed zone at elevation -146 to -262 masl and -574 to -853 masl, there are faults and some continuous conductive fracture that are responsible to the flow contribution (see the fracture density chart). The fault on elevation around -207 masl is also responsible to the total loss circulation.

3.2 Well K

From the chart below (Figure 5), we can infer that the well is also influenced by NW-SE fractures. These fractures are dominated by SW dip azimuth from elevation -350 to -650 masl, while the SE dip azimuth intensity starts from elevation -650 masl downward. Around elevation -600 to -650 masl a deflected temperature profile is observed. It is indicated that the main feed zones with numerous conductive fractures around that elevation are responsible for it. It is noticeable that from elevation -800 to -900 masl around 40% flow contribution is concentrated there due to intensive fracturing. Meanwhile, the rest flow contribution (60%) is distributed on the upper part with 500 m thick.

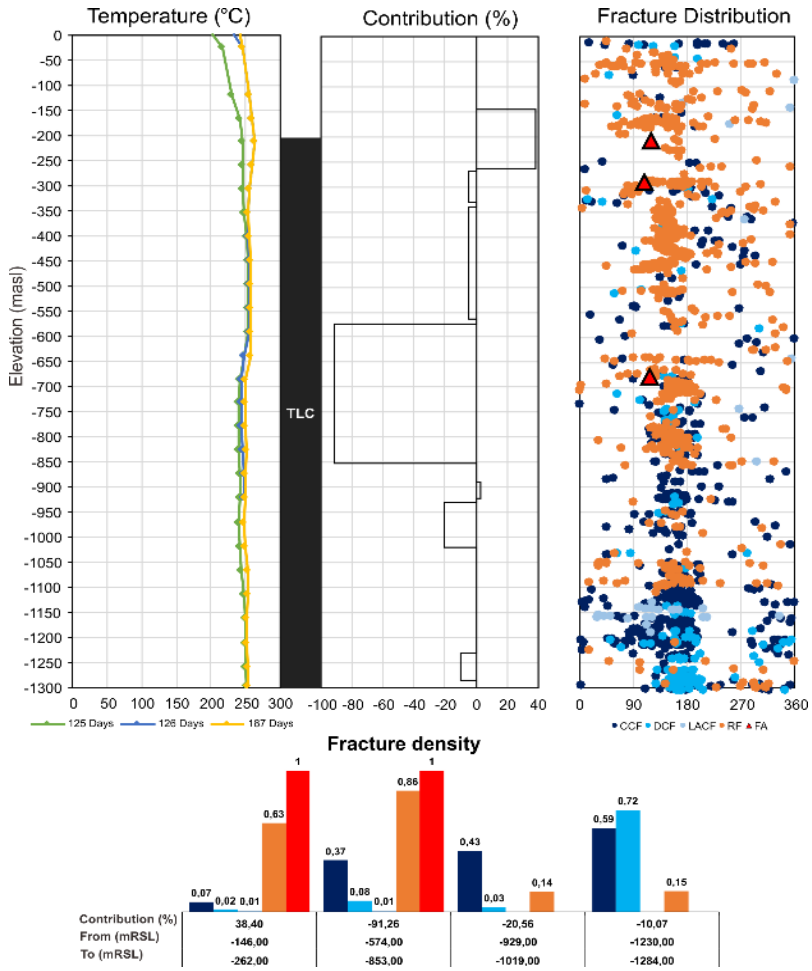

Figure 4: Temperature, drilling circulation, flow contribution, fracture distribution and fracture density of Well B. Notice that the start of TLC coincides with the fault.

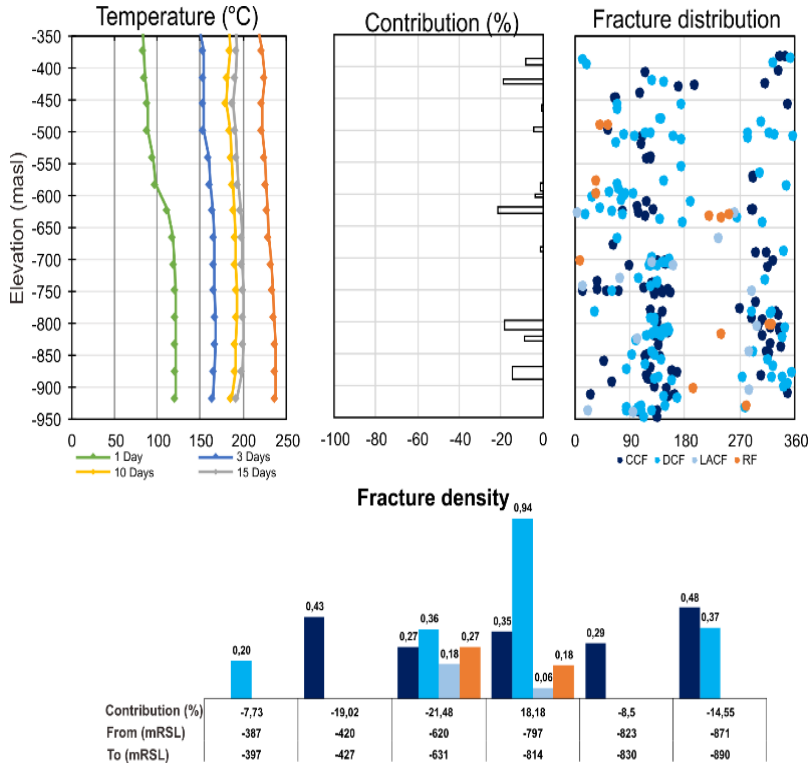

Figure 5: Temperature, flow contribution, fracture distribution and fracture density of Well K. No loss circulation found, only partial. Feed zones from -800 to -900 masl contribute to 40% flow.

3.3 Well H

This well is similar to others, dominated by NW-SE fractures from top to bottom of the logged interval, with NE-SW as the subordinate (Figure 6). The increasing intensity of conductive fractures is correlated with the progression of mud circulation losses from intermittent to fully total at around -380 to -490 masl and sharp temperature deflection (-500 to -600 masl). The deflected temperature profile is controlled by the main feed zone (80% contribution) on elevation -540 to -600 masl where it contains a lot of conductive fractures (CCF, DCF, LACF) with very minor resistive fracture. Besides that, there are numerous wide open fracture (20 – 25 cm) found in this interval (Figure 7). Resistivity fractures intensity increases just after the main feed zone. The second and smaller feed zone is contributed from less intense conductive fractures, accumulating 20% contribution.

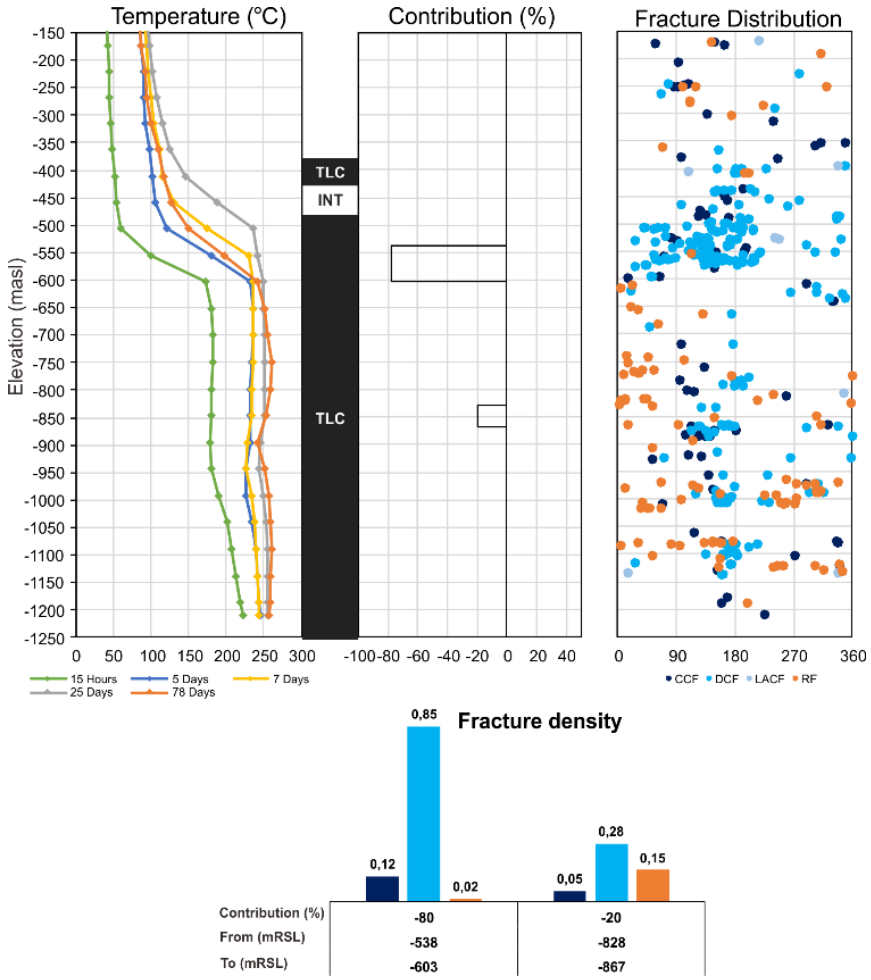

Figure 6: Temperature, drilling circulation, flow contribution, fracture distribution and fracture density of Well H. Sharp deflection on temperature correlates with the first feed zone around -540 to -600 masl.

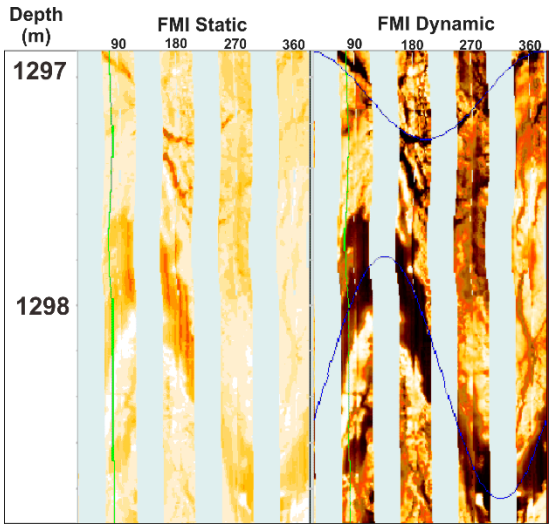

Figure 7: Widely open continuous conductive fracture in Well H that contributes as the major feed zone.

3.4 Well D

The logged borehole image data could only be obtained up to elevation -1000 masl while the feed zones are deeply located starts from elevation -905 masl downward. So we are limited to discuss only at the covered zone which covers half of the first feed zone (Figure 8). The fractures itself dominate the well with NW-SE strike and NE dip azimuth that contains discontinuous conductive fractures, resistive fractures with less conductive continuous fractures and the low angle conductive fractures. When the resistive fractures decreases at elevation -900 masl, while at the same time entering the first feed zone, temperature profile increases and turns to convective profile at elevation -1030 masl. In the half of first feed zone, the fractures are dominated by discontinuous conductive fracture with 0,65 fracture/m. Within this first feed zone, we found a break in circulation while drilling that caused TLC for a while and then became total loss around elevation -1000 masl.

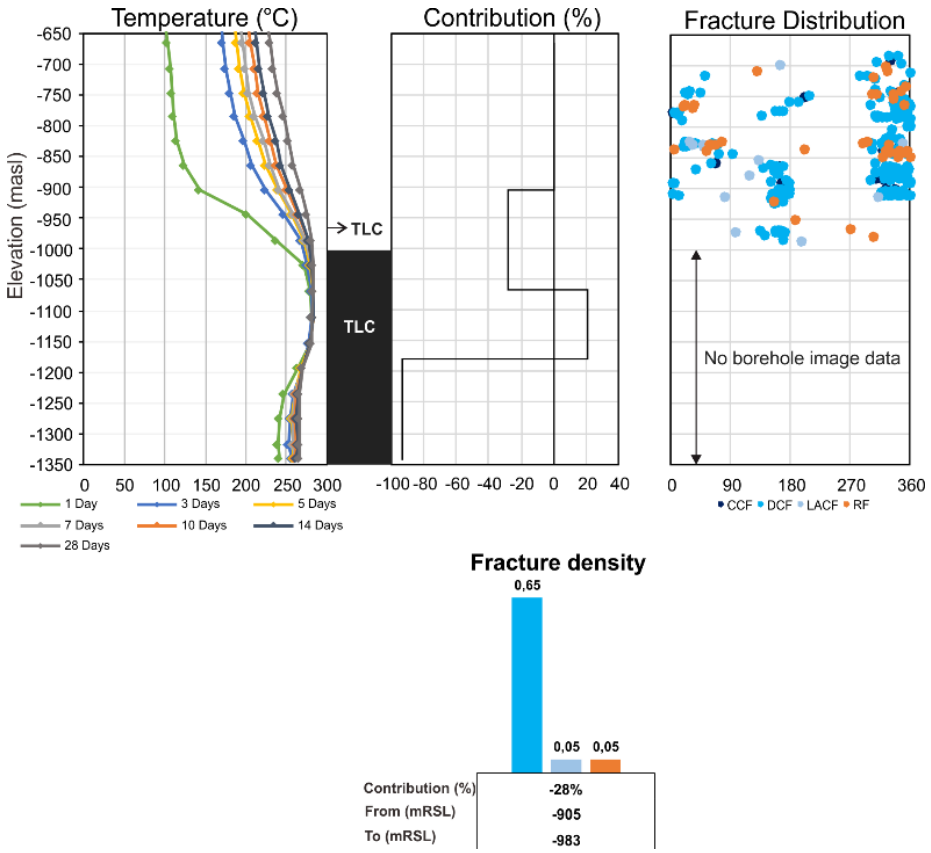

Figure 8: Temperature, drilling circulation, flow contribution, fracture distribution and fracture density of Well D. The TLC zone coincides with convective temperature profile with major flow contribution that indicates good permeable structure although there is no borehole image data.

3.5 Well R1

In general, the well is dominated by NW-SE fractures consisting of discontinuous conductive fracture with minor continuous conductive fractures (Figure 9). At the top of the logged interval, the minor feed zone at elevation -160 masl caused total loss circulation for several minutes. Later on the drilling circulation became intermittent along with two feed zones containing some continuous conductive fractures.

Total loss circulation occurred from elevation -440 masl downward. At the same elevation, the temperature profile shows convective profil. Within the TLC interval, the fracture intensity increases sharply and there is a major feed zones with 70% contribution at elevation of -560 masl due to fault (Figure 3D). The fractures become more intense with NW-SE strike and NE or SW dip azimuth. Around 80% flow contribution is located within this TLC interval.

3.6 Well R2

The well is a vertical well as we can see on Figure 2. It is dominated by NW-SE fractures with either dipping to NE or SW with NE-SW as the subordinate fractures (Figure 10). Intense fractures distribution occurs at depth between -650 to -1200 masl. In this interval there are several minor feed zones that counts up to 20% flow contribution within this 550 m thick interval. There were two occasions when the drilling intersected total circulation loss zone and both are within above interval.

Around elevation -1200 masl downward, total loss circulation occurred and there is a deflected profile temperature. Within this TLC interval, nearly 80% flow contribution comes from 4 (four) feed zones. The largest one is at the elevation -1230 masl. Near this depth, the borehole image data failed to record the image for 5 m length due to washed out borehole. It is possibly caused by intensive fracturing or faulting occurred at the washed out interval.

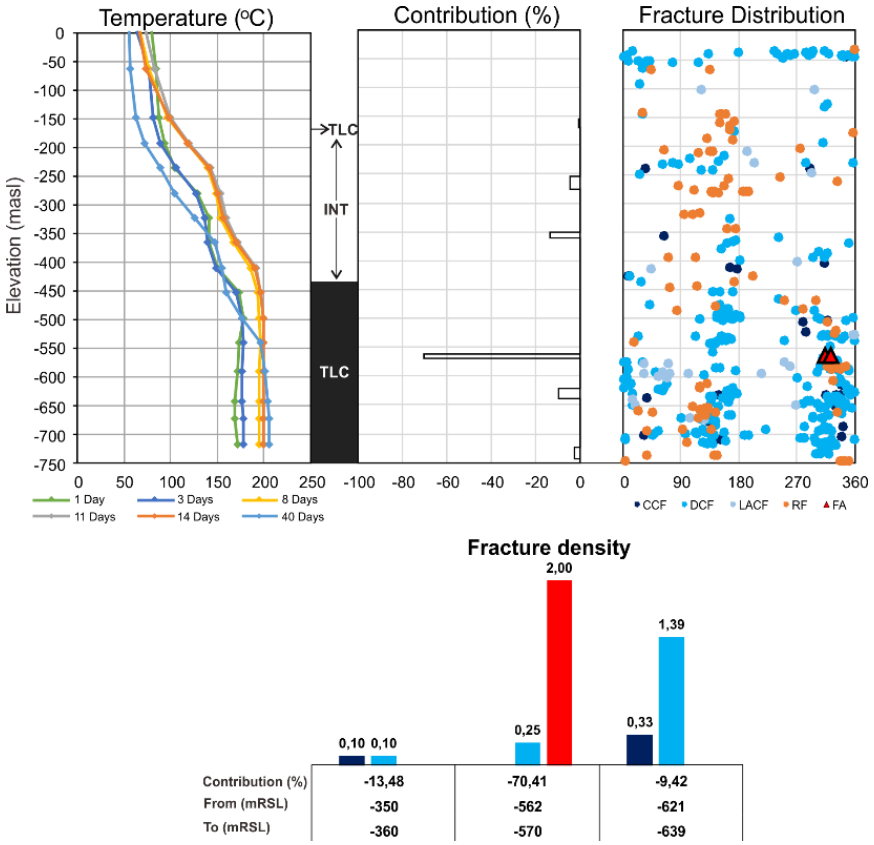

Figure 9: Temperature, drilling circulation, flow contribution, fracture distribution and fracture density of Well R1. Fault on elevation -560 masl contributes to the 70% flow. The TLC zone coincides with the convective temperature profile.

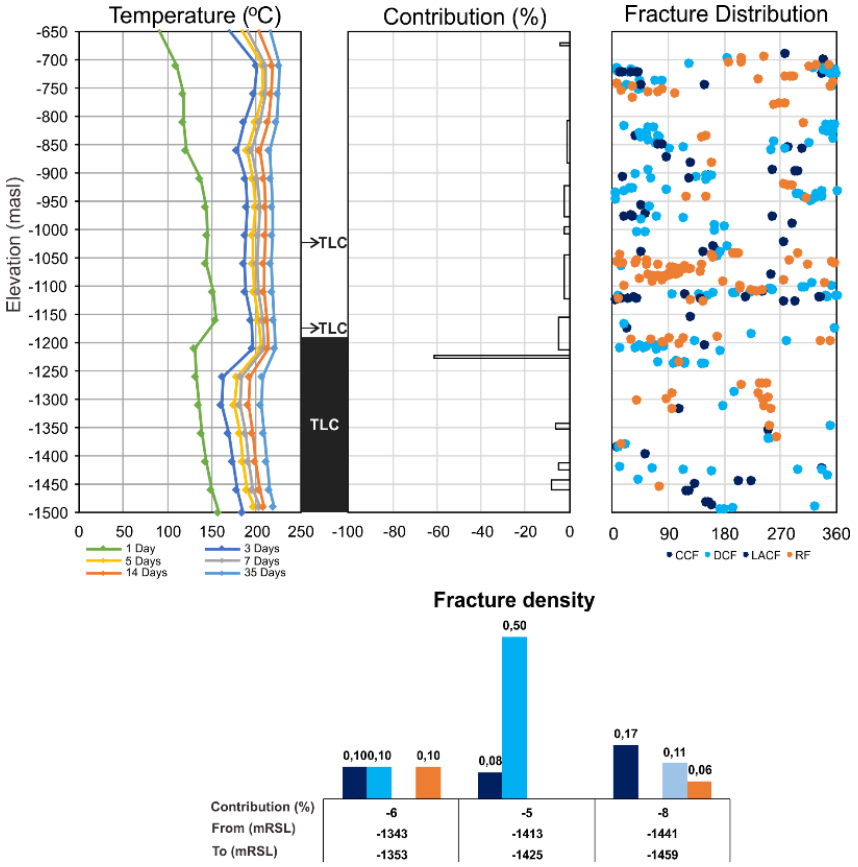

Figure 10: Temperature, drilling circulation, flow contribution, fracture distribution and fracture density of Well R1. It is interpreted that major feed zone in elevation -1230 masl is contributed by fault.

3.7 Fracture density vs flow contribution

The study above reveals that the more intense or dense the conductive fractures (including CCF, DCF, LACF and fault) in a well, the greater the flow contribution. The resistive fracture is excluded from this assumption as it is interpreted that the fractures are filled by resistive minerals such as calcite, quartz, etc. and does not contribute to the flow.

Plotting the fracture density against the flow contribution from each feed zones gave insight about how much the influence of fault and conductive fractures to the flow contribution (Figure 11). In this calculation, faults are excluded from the calculation and count as 1.

It is observed that there are 4 (four) ranks of feed zone based on the fault and conductive fracture density. The first one is when the feed zone has <0,6 conductive fractures/m, the flow contribution only counts as maximum as 20%. Second, when the density is > 0,6 conductive fractures/m, the flow contribution is as minimum as 10%. Third, at the 1st feed zone in Well K, 80% flow contribution is due to the occurrence of widely open conductive fractures as seen on Figure 7. Fourth, flow contribution increases significantly if the fault intersect the wells such as in Well B, Well D and Well R2.

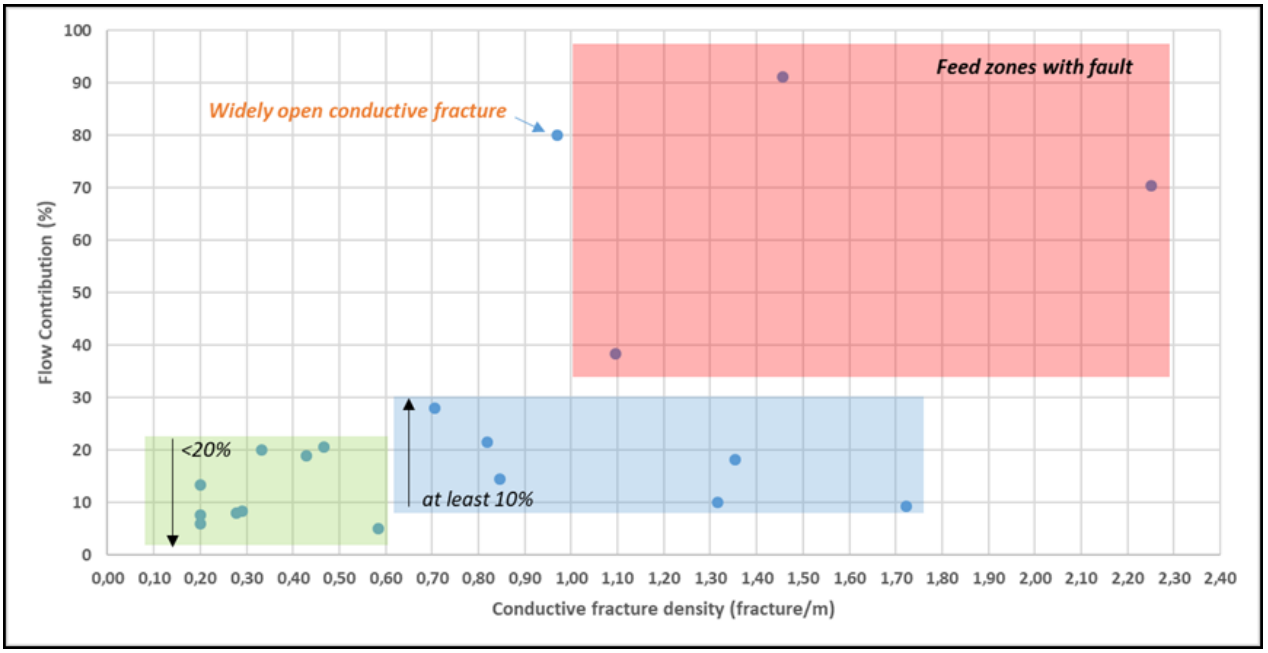

Figure 11: Conductive fracture density including CCF, DCF, and LACF and fault which is count as 1 plotted against flow contribution. Four feed zones rank are made; (1) Feed zones with <0,6 conductive fracture density (translucent green box); (2) Feed zones with >0,6 conductive fractures density without fault (translucent blue box); (3) Feed zones with widely open conductive fractures (orange text); (4) Feed zones with fault (translucent red box).

3.8 Feed zone characterization and its application to the field development

By plotting the feed zone with its flow contribution and elevation in a bubble chart (Figure 12), it is observed that feed zones from the wells on the western part and the eastern part behave differently. Wells in the western part have major feed zone starting from elevation -146 to around -574 masl. Meanwhile, the eastern part of the field, major feed zone is found deeper starting from elevation around -1179 to -1221 masl. The feedzones due to fault (red bubble) are located on the same elevation in each eastern and western zones. It is interpreted that the wells in each zones penetrated the same fault zones at the same elevation.

Well B succeeded to penetrate elevation of -1200 masl, the flow contribution in this depth is quite small (only 10% contribution). Furthermore, Well H also reached to elevation around -1250 masl and found no feed zone at this depth. On the eastern part, due to hole problem Well K could not reach the elevation deeper than -1000 masl. Practically for future field development, there is no urgency to drill deeper than -1000 masl in the western part to target the main feed zones. On the other side, the drilling program in the eastern part must achieve the elevation up to -1250 masl to reach the productive target.

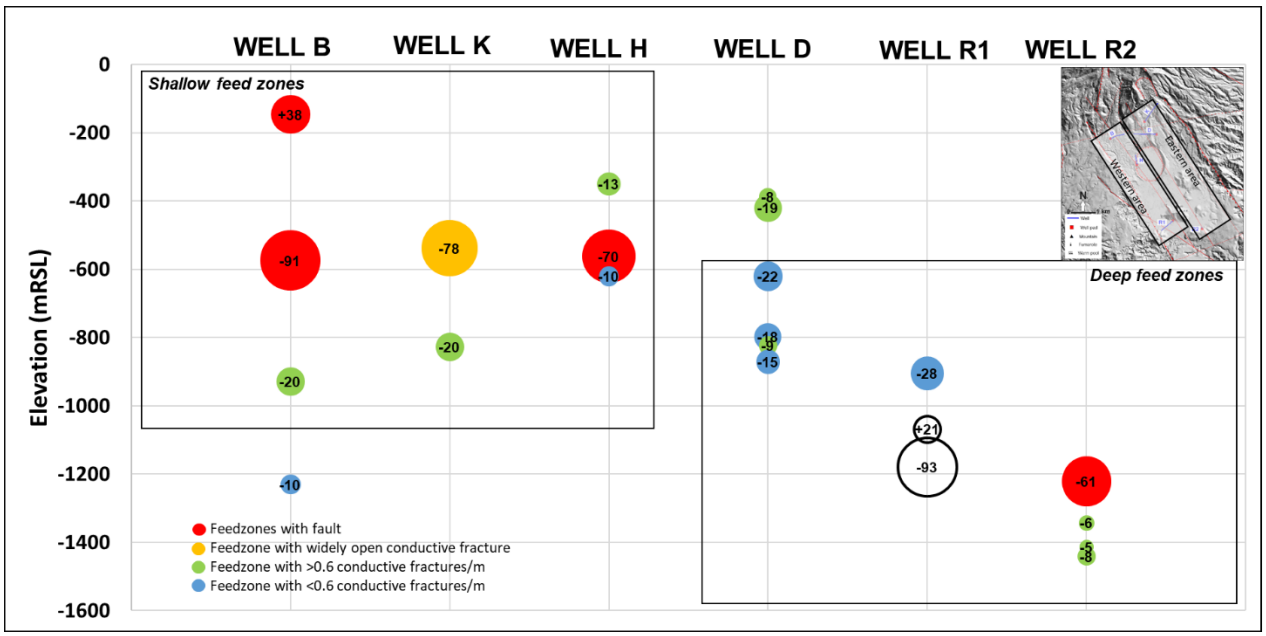

Figure 12: Feed zone distribution across the wells and its rank based on the fault and conductive fracture density. Note that the western part of the field is shallower than the feed zones in the eastern part (see map on Figure 2 to see the location of the wells). The bubble is coloured based on the rank on Figure 11. Bubble size reflects the flow contribution. The numbers within the bubble is the percentage of the flow, plus sign is an inflow from formation to the borehole, minus sign is an outflow from the borehole to the formation.

3.9 Feed zone distribution and its controlling factor

In figure 13, it is noticed that the feed zones are predominantly covered within the rhyolitic tuff as the feed zones are identified below the top of rhyolitic tuff (Top RT). Within this interval, both of partial and the latter total loss circulation were occurred during drilling phase. Rhyolitic tuff is interpreted as a pyroclastic flow deposit of immersive eruption that fills the depression of Ulubelu (ignimbrite). It is characterized by white, creamy, light greyish coloured, mainly composed of altered volcanic glass, tuff, quartz, and feldspar crystal fragments as found in cuttings and core from Ulubelu wells. Hydrothermal alteration in this unit shows both matrix and fractures/veins deposit of quartz-epidote-pyrite (Figure 14). This pervasive deposit of alteration minerals depicts that along with the primary bulk permeability from their natural grainy texture, the secondary permeability from faults and fractures also enhance the already porous and permeable rhyolitic tuff. The hydrothermal alteration processes at the same time follow the rock unit. Beneath this rhyolitic tuff rock unit lies the metasediment. This unit is impenetrable for drilling and the top of metasediment acts as the base of productive zones of Ulubelu Geothermal Field.

The major feedzones in the field are located differently, it sits at deeper elevation in the in eastern part than in the western part. Stratigraphic offset of rhyolitic tuff is also observed between the wells in the western part (Well B, Well H, Well R1) and the wells in the eastern part (Well K, Well D, Well R2). The top RT in the western part is shallower than in the eastern part although in Well H and Well R1 shows slightly occurrence of rhyolitic tuff. In addition, the occurrences of top RT precedes the total loss circulation. This stratigraphic offset of rhyolitic tuff is interpreted as the result of structural control that formed the Ulubelu depression. Therefore, feed zones in Ulubelu Geothermal Field are controlled by the structure beneath it and also must be within or below the rhyolitic tuff unit where it provides bulk matrix permeability and also its secondary permeability.

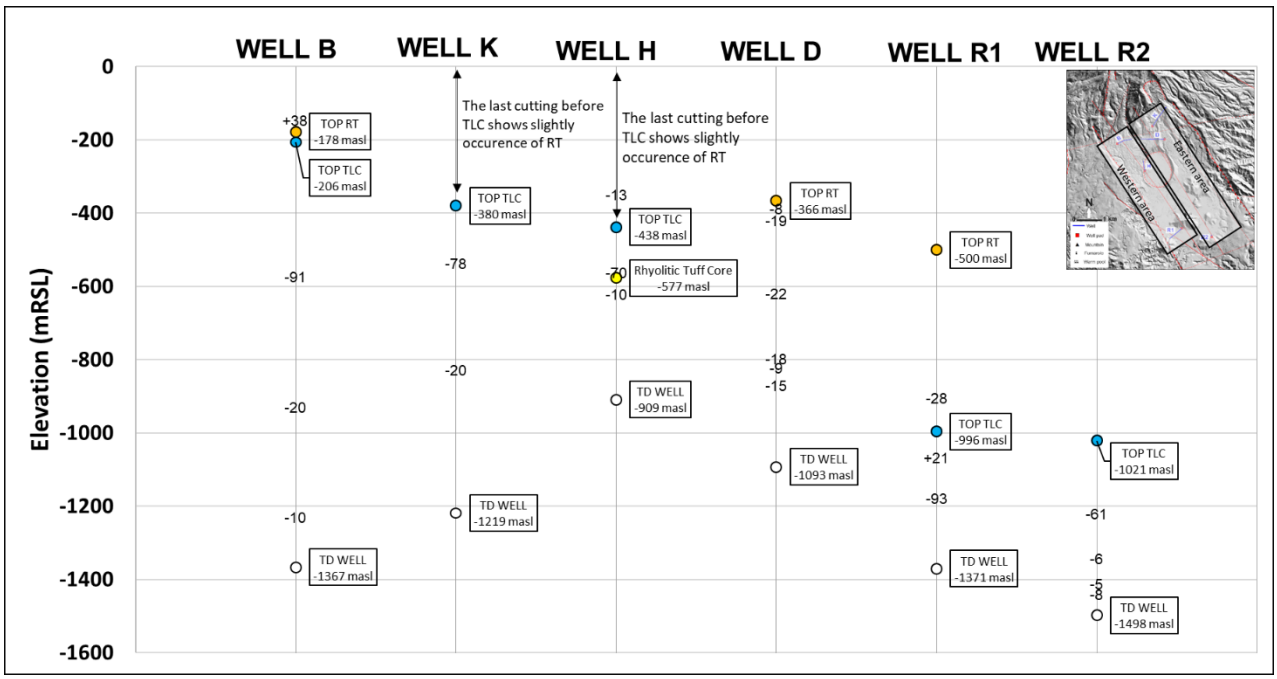

Figure 13. Feed zones distribution along with top of rhyolitic tuff (Top RT), top total loss circulation (Top TLC) and total depth of each well (TD Well). There is a stratigraphic offset of Top RT between wells in the western (Well B, Well H, Well R1) and eastern part (Well K, Well D, Well R2). This top RT precedes the Top TLC.

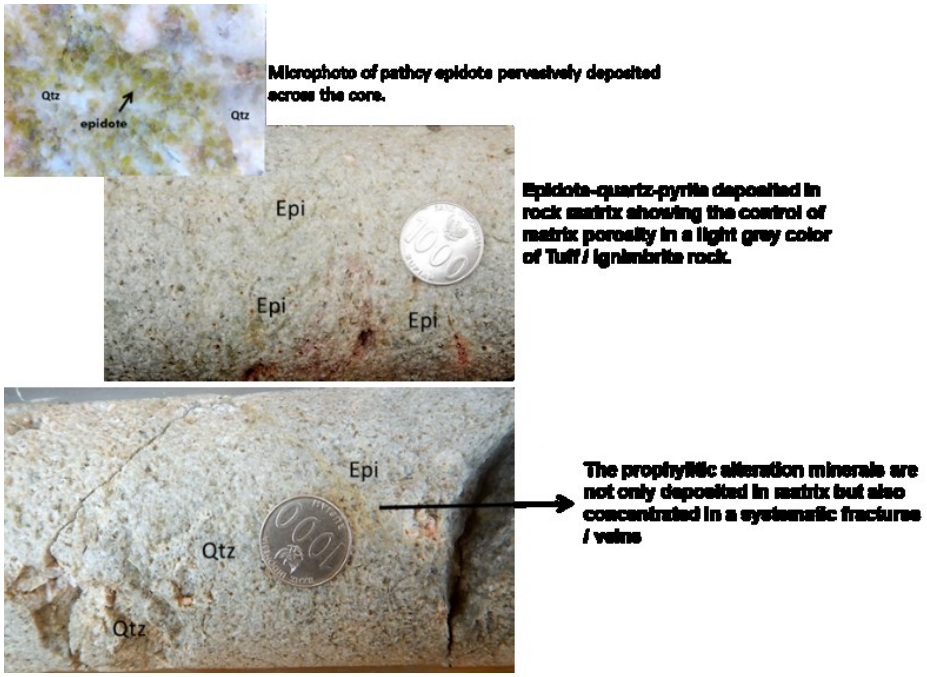

Figure 14. Evidence of pervasive matrix deposit and veins of Epidote in rhyolitic tuff (Internal report PGE, 2018)

4. CONCLUSION

Based on the surface data, the UGF is dominated by NW-SE structures. The trend is also consistent with the subsurface data as shown on the fractures distribution from this study. The NW-SE structures, comprised of conductive fractures (CCF, DCF, LACF) and faults, intersected by the wells are mainly responsible to the geothermal fluid flow contribution. The more intense distribution of conductive fractures in the feed zone, the greater the flow contribution. Besides structural control, lithological control also contributes to the feedzone distribution. It is observed that most feedzones are located within the rhyolitic tuff unit where it has natural bulk primary permeability and also the secondary permeability from fracturing. Thus, identification of feed zones controlling factor and relatively quantifying the contribution of faults and fractures will greatly assist the future field development and plan the effective make-up wells.

REFERENCES

Barber, A.J., Crow, M.J., and Milsom, J.S., Sumatra: Geology, Resources and Tectonic Evolution. Geological Society, London, Memoirs, 31 (2005), 290 pp.

Darman, H., and Sidi, F.H., 2000, An Outline of the Geology of Indonesia, Indonesian Association of Geologists, Jakarta, 192pp.

Exploitation Geoscience and Reservoir Engineering Team (EGRE Team), 2018, Ulubelu Geothermal Field Conceptual Model Update, Internal Report PGE, Jakarta.

Muraoka, H., Takahashi, M., Sundhoro, H., Dwipa, S., Soeda, Y., Momita, M., and Shimada, K., 2010, Geothermal Systems Constrained by The Sumatran Fault and Its Pull-Apart Basins in Sumatra, Western Indonesia, Proceedings World Geothermal Congress, Bali, Indonesia, 25-29 April.

Sieh, K. And Natawidjaja, D., 2000, Neotectonics of the Sumatran fault, Indonesia. Journal of Geophysical Research.

Trianggo, S., Sardiyanto, Koestono, H., Thamrin, M.H., Kamah, M.Y., 2015, Evaluation of The Productive Geological Structure in Ulubelu Geothermal System, Proceedings World Geothermal Congress, Melbourne, Australia, 19-25 April.